Title

The WNT receptor FZD7 is required for maintenance of the pluripotent state in human embryonic stem cells

Journal

Proceedings of the National Academy of Sciences of the United States of America, 111(4)

ISSN

0027-8424

Authors

Fernandez, Antonio
Huggins, Ian J
Perna, Luca
et al.

Publication Date

2014-01-28

DOI

10.1073/pnas.1323697111

Peer reviewed

The WNT receptor FZD7 is required for maintenance of the pluripotent state in human embryonic stem cells

Antonio Fernandez[a,1], Ian J. Huggins[a,1], Luca Perna[a], David Brafman[a], Desheng Lu[b,2], Shiyin Yao[b], Terry Gaasterland[c], Dennis A. Carson[b,3], and Karl Willert[a,3]

[a]Department of Cellular and Molecular Medicine, Stem Cell Program, University of California, San Diego, La Jolla, CA 92093-0695; [b]Rebecca and John Moores Cancer Center, Sanford Consortium for Regenerative Medicine, University of California, San Diego, La Jolla, CA 92093; and [c]Scripps Institution of Oceanography and Institute for Genomic Medicine, University of California, San Diego, La Jolla, CA 92093-0202

Contributed by Dennis A. Carson, December 20, 2013 (sent for review October 15, 2013)

WNT signaling is involved in maintaining stem cells in an undifferentiated state; however, it is often unclear which WNTs and WNT receptors are mediating these activities. Here we examined the role of the WNT receptor *FZD7* in maintaining human embryonic stem cells (hESCs) in an undifferentiated and pluripotent state. *FZD7* expression is significantly elevated in undifferentiated cells relative to differentiated cell populations, and interfering with its expression or function, either by short hairpin RNA-mediated knockdown or with a fragment antigen binding (Fab) molecule directed against FZD7, disrupts the pluripotent state of hESCs. The FZD7-specific Fab blocks signaling by Wnt3a protein by down-regulating FZD7 protein levels, suggesting that FZD7 transduces Wnt signals to activate Wnt/β-catenin signaling. These results demonstrate that *FZD7* encodes a regulator of the pluripotent state and that hESCs require endogenous WNT/β-catenin signaling through FZD7 to maintain an undifferentiated phenotype.

human pluripotent stem cell | self-renewal | differentiation

Control of stem cell self-renewal is critical to the development of multicellular life; however, our understanding of the molecular machinery regulating this process remains superficial. Several studies have demonstrated that the WNT/β-catenin signaling pathway is a critical regulator of stem cell self-renewal, and the hypothesis that WNT primarily acts to maintain stem cells in an undifferentiated state has garnered significant support (reviewed in refs. 1–4). This paradigm is especially apparent in various adult stem cell populations, such as in skin, intestine, and blood, where WNT/β-catenin signaling is essential for proper tissue homeostasis.

The role of WNT signaling in embryonic stem cells has been more controversial. In mouse embryonic stem cells, WNT/β-catenin signaling is active, and its inhibition shifts cells into an epiblast-like state (5–9). In contrast, in human embryonic stem cells (hESCs), which more closely resemble mouse epiblast stem cells than mouse embryonic stem cells (10, 11), WNT/β-catenin signaling is largely inactive, and ectopic stimulation of the pathway shifts them toward mesendodermal fates (12–14).

Confounding the analysis of the role of WNT signaling in pluripotent stem cells is the large number of WNT ligands (the mammalian genome contains 19 *Wnt* genes) and WNT receptors encoded by the *FZD* gene family (the mammalian genome contains 10 *Fzd* genes), some of which may be acting redundantly. Furthermore, relatively little is known about the specificities of individual WNTs for individual receptors. Here we describe a set of experiments that demonstrate the presence of an endogenous WNT-FZD signaling loop that mediates a self-renewal signal in hESCs.

Results

Previous studies showed that *Fzd7* is expressed in the epiblast of the developing mouse embryo (15) and that the human homolog *FZD7* is elevated in undifferentiated human embryonic stem cells (hESCs) (16, 17). We extended these studies by determining relative expression levels of all 10 *FZD* genes in hESCs using a whole-transcriptome sequencing (RNA-seq) data set. This analysis demonstrated that *FZD7* is the most abundantly expressed *FZD* gene in the hESC line H1/WA01 (Fig. 1*A*). Levels of the second and third most highly expressed *FZD* genes, *FZD5* and *FZD3*, were 4.2-fold and 8.8-fold lower, respectively. That *FZD7* is the most abundantly expressed *FZD* gene was confirmed using quantitative reverse transcription PCR (qRT-PCR) in a separate hESC line, HUES9 (Fig. S1*A*). On differentiating hESCs to fibroblasts by withdrawal of the self-renewal signal fibroblast growth factor 2 (FGF2), expression levels of *FZD7* declined significantly (Fig. 1*B*). Similarly, on reprogramming of fibroblasts to an induced pluripotent state, *FZD7* expression was increased (Fig. S1*B*). Using previously published protocols (18), we differentiated hESCs (HUES9) into each of the three germ layers and monitored expression of all 10 *FZD* genes in each cell population relative to undifferentiated hESCs (Fig. 1*C* and Fig. S1*C*). We found that *FZD7* expression was down-regulated in all differentiated cell populations relative to undifferentiated cells (Fig. 1*C*). Differentiation into each lineage was monitored by expression of lineage-specific genes: *SOX1* for ectoderm, *T* (*brachyury*) for mesoderm, and *SOX17* for endoderm (Fig. 1*C*). Given the consistent correlation of *FZD7* gene expression with the pluripotent state, we performed additional experiments to address *FZD7*'s functional importance in pluripotent stem cells.

Significance

Embryonic stem cells (ESCs) are unique in their ability to expand and self-renew indefinitely while retaining the potential to give rise to all mature cell types. The molecular mechanisms underlying these properties remain poorly understood. We investigated the role of the highly conserved WNT signaling pathway in controlling self-renewal and found that the WNT receptor encoded by the frizzled family receptor 7 (*FZD7*) gene is essential for maintaining human ESCs in an undifferentiated and pluripotent state. Using an FZD7-specific fragment antigen binding protein, as well as knockdown of FZD7 expression, we showed that the FZD7 receptor transduces a WNT/β-catenin signal in human ESCs. These data demonstrate that an endogenous WNT signaling loop is essential for the maintenance of human ESCs in an undifferentiated state.

Author contributions: K.W. designed research; A.F., I.J.H., L.P., D.B., D.L., S.Y., and K.W. performed research; D.A.C. contributed new reagents/analytic tools; A.F., I.J.H., T.G., and K.W. analyzed data; and K.W. wrote the paper.

The authors declare no conflict of interest.

Freely available online through the PNAS open access option.

[1]A.F. and I.J.H. contributed equally to this work.

[2]Present address: Shenzhen University Cancer Research Center, Shenzhen 518060, China.

[3]To whom correspondence may be addressed. E-mail: kwillert@ucsd.edu or dcarson@ucsd.edu.

This article contains supporting information online at www.pnas.org/lookup/suppl/doi:10.1073/pnas.1323697111/-/DCSupplemental.

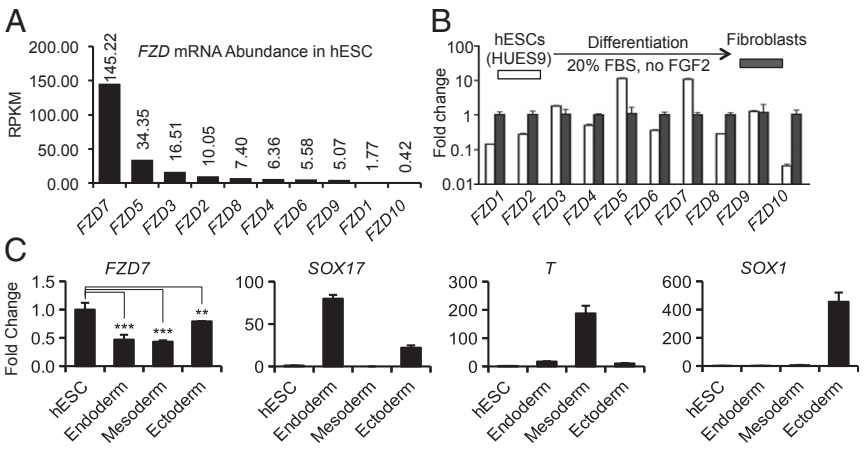

Fig. 1. Characterization of *FZD7* expression. (*A*) *FZD7* is the most abundantly expressed *FZD* gene in hESCs. Gene expression levels for all 10 *FZD* genes were calculated from RNA-seq data as reads per thousand transcript bases per million reads mapped (RPKM). (*B*) *FZD7* expression is down-regulated on differentiation of hESCs to fibroblasts. hESCs were differentiated to fibroblasts in 20% (vol/vol) FBS and in the absence of the self-renewal factor FGF2. Data are represented as mean ± SD of three technical samples, normalized to *EF1a* and relative to fibroblasts. (*C*) *FZD7* expression is down-regulated on differentiation into ecto-, endo-, and mesoderm. hESCs were treated to differentiate into one of the 3 germ layers. Acquisition of a differentiated phenotype was determined by expression of *SOX17* (endoderm), *T* (*BRY*, mesoderm), and *SOX1* (ectoderm). *FZD7* data are presented as mean ± SD of two biological replicates with four technical replicates each. $^{**}P < 0.01$; $^{***}P < 0.001$.

To further characterize the role of FZD7 in hESCs, we tested a FZD7-specific fragment antigen binding (Fab) protein for its ability to bind FZD7, from here on referred to as FZD7-Fab. This Fab reacted with FZD7 overexpressed in HEK293 cells by immunoblotting (Fig. 2*A*). Other members of the FZD protein family, including the two most similar FZDs, FZD1 (79% identical to FZD7) and FZD2 (80% identical to FZD7), were not recognized by FZD7-Fab (Fig. 2*A*). By flow cytometry, FZD7-Fab effectively bound the cell surface of live HEK293 cells transiently transfected with a FZD7 expression vector (Fig. 2*B*). FZD7-Fab also specifically recognized a protein in hESCs (HUES9) of similar molecular mass, as observed in HEK293 cells transfected with a FZD7 expression vector (Fig. 2*C*), demonstrating that this Fab detects endogenously expressed FZD7 protein. Staining of live hESCs with FZD7-Fab followed by flow cytometry indicated that a large percentage of cells displayed this receptor on the cell surface (Fig. 2*D* and Fig. S2). Fluorescence-based cell sorting to obtain cell populations with either high or low cell surface staining of FZD7 ($FZD7^{hi}$ or $FZD7^{lo}$), followed by qRT-PCR, demonstrated that FZD7-Fab can be used to enrich cells with higher levels of *FZD7* expression (Fig. 2*E*). Furthermore, the $FZD7^{hi}$ population expressed significantly higher levels of the pluripotency markers *NANOG* (Fig. 2*E*). Therefore, FZD7 marks hESCs with higher levels of expression of pluripotency-associated genes, such as *NANOG*.

To explore the functional importance of FZD7 in undifferentiated hESCs, we took two approaches to disrupt its function: delivery of short hairpin RNA (shRNA) to knock down its

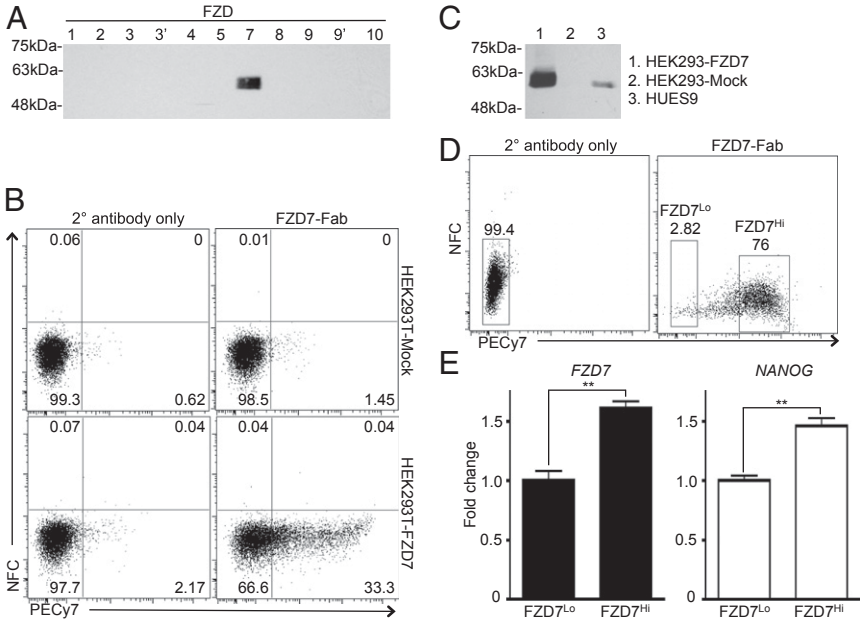

Fig. 2. Characterization of FZD7 protein. (*A*) FZD7-Fab specifically recognizes FZD7 protein by immunoblotting. HEK293 cells were transiently transfected with expression vectors containing the indicated *FZD* genes. FZD3′ and FZD9′ represent truncated versions of the full-length genes. An expression vector carrying *FZD6* was not available for these experiments. (*B*) FZD7-Fab reacts with FZD7 protein on live HEK293 cells by flow cytometry. Untransfected cells and secondary (2°) antibody alone served as negative controls. NFC, nonfluorescent channel. (*C*) FZD7-Fab specifically reacts with a protein in HUES9 cells of the same molecular mass as overexpressed FZD7. Cell lysates from FZD7 transfected HEK293 cells (lane 1), mock-transfected HEK293 cells (lane 2), and HUES9 cells (lane 3) were immunoblotted with FZD7-Fab. (*D*) FZD7-Fab specifically reacts with an antigen displayed on live HUES9 cells. (*E*) Using fluorescence-based cell sorting, hESCs (HUES9) were separated into cell populations with high levels ($FZD7^{Hi}$) and low levels ($FZD7^{Lo}$) of FZD7 on the cell surface. qRT-PCR analysis revealed that expression of the pluripotency marker NANOG and FZD7 itself was significantly enriched in the $FZD7^{Hi}$ population (mean ± SD of three technical samples, normalized to 18S and relative to FZD7 low populations). $^{**}P < 0.01$.

expression (Fig. 3) and application of FZD7-Fab to block its function (Fig. 4). shRNAs were delivered using lentiviral transduction, and knockdown efficiency was determined for five independent shRNAs (Fig. S3*A*). In support of our finding that hESCs with the highest FZD7 expression retain the highest levels of pluripotency marker expression (Fig. 2*E*), we observed a direct correlation between the extent of *FZD7* knockdown and reduction in expression of *NANOG* and *POU5F1*/*OCT4* (Fig. S3*A*). Knockdown of *FZD7* was accompanied by a loss in characteristic hESC morphology (colonies with sharp boundaries) and acquisition of a fibroblast-like morphology (Fig. 3*A* and Fig. S3*D*), as well as a significant reduction in expression of the pluripotency regulators *NANOG* and *POU5F1*/*OCT4* in HUES9 cells (Fig. 3*B*) and HUES6 cells (Fig. S3 *B* and *C*). Therefore, disrupting *FZD7* expression impairs the pluripotent state of hESCs.

Because FZD7-Fab specifically bound FZD7 protein on the surface of hESCs, we reasoned that it could potentially antagonize FZD7 function. To address this possibility, we examined the effect of prolonged treatment of hESCs with FZD7-Fab. Cells treated with FZD7-Fab showed a significant reduction in expression of the pluripotency markers *OCT4*/*POU5F1* and *NANOG* (Fig. 4*A* and Fig. S4*A*), indicating that blocking FZD7 function impairs growth of hESCs in an undifferentiated state. This treatment, similar to the knockdown of *FZD7* with shRNA, led to a reduction in expression of the *FZD7* gene itself, an observation consistent with the notion that FZD7 is not only a marker of undifferentiated cells but also is functionally important for the maintenance of hESCs in an undifferentiated state.

Although FZD7-Fab treatment impaired expression of pluripotency-associated genes, it did not interfere with differentiation of hESCs into the mesendodermal lineage, an effect mediated by

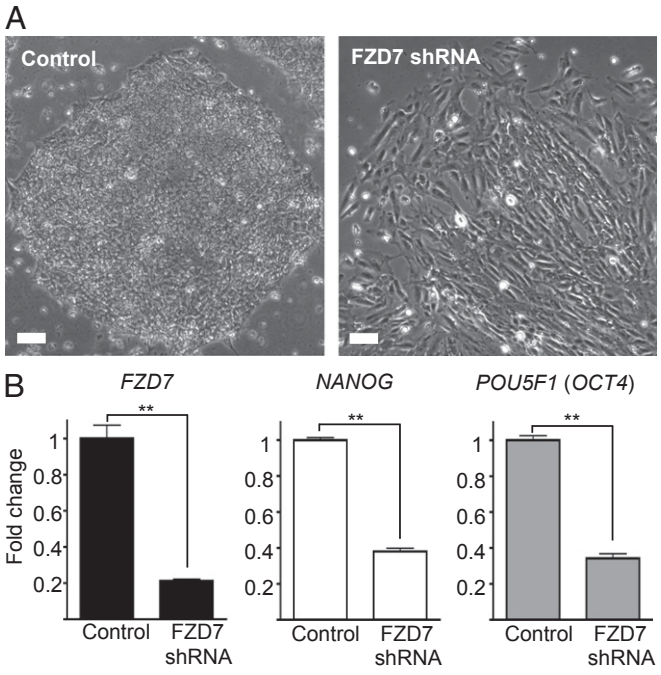

Fig. 3. Disruption of *FZD7* expression impairs the pluripotent state of hESCs. (*A*) Knockdown of *FZD7* expression in hESCs (HUES9) results in the loss of characteristic hESC morphology (tightly packed colonies with sharply demarcated boundaries). (Scale bar, 100 μm.) (*B*) *FZD7* depletion by shRNA knockdown leads to a reduction of pluripotency gene expression. hESCs transduced with a shRNA directed against *FZD7* exhibited a significant decline in expression of the genes *FZD7*, *NANOG*, and *POU5F1*/*OCT4* (mean ± SD of three technical samples, normalized to *EF1a* and relative to mock-infected controls). $^{**}P < 0.01$.

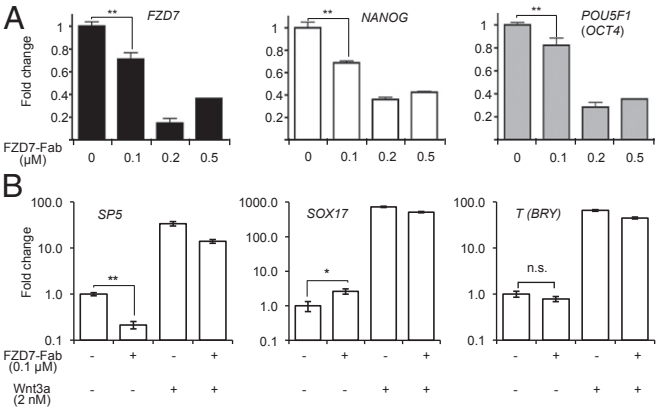

Fig. 4. Disruption of FZD7 function impairs hESC pluripotency, but not mesendodermal differentiation. (*A*) Treatment of hESCs with FZD7-Fab reduces expression of genes associated with the pluripotent state. hESCs were cultured for 3 passages in the presence of the indicated concentrations of FZF7-Fab. At the end of this treatment, expression of *FZD7*, *NANOG*, and *POU5F1*/*OCT4* was determined by qRT-PCR (mean ± SD of three technical samples, normalized to 18S and relative to buffer control). $^{**}P < 0.01$. (*B*) Treatment of hESCs with FZD7-Fab does not interfere with Wnt3a-induced mesendodermal differentiation. hESCs were treated with purified Wnt3a in the presence or absence of FZD-Fab at the indicated concentrations. After 5 d of treatment, expression of *SP5*, *SOX17*, and *T (BRY)* was determined by qRT-PCR (mean ± SEM of four technical samples, normalized to 18S and relative to buffer control). $^{**}P < 0.01$; $^{*}P < 0.05$; n.s. not statistically significant.

canonical WNT signaling (12). Cells treated with exogenous Wnt3a protein down-regulate pluripotency-associated genes and enter a mesendodermal fate, as detected by the expression of *SOX17* and *T* (*BRY*; Fig. 4*B*). Cotreatment with FZD7-Fab did not significantly affect up-regulation of *SOX17* and *T* expression, suggesting that FZD7 does not mediate mesendodermal differentiation. In contrast, expression of the WNT target gene *SP5* was significantly reduced on treatment with FZD7-Fab. Together, these data suggest that FZD7 mediates an endogenous WNT signaling loop that maintains baseline expression of the WNT target gene *SP5* and expression of the pluripotency-associated genes *OCT4*/*POU5F1* and *NANOG* but does not participate in mesendodermal differentiation.

Because the primary known function of FZD proteins is to transduce WNT signals, we explored the possibility that FZD7 transduces Wnt signals to activate β-catenin-mediated transcription. As a first measure, we interrogated RNA-seq data to identify expression of *WNT* genes in hESCs. Consistent with other studies (14) and publically available expression data sets [e.g., the Gene Expression Atlas, www.ebi.ac.uk/gxa/ (19)], *WNT3* was expressed in hESCs (Fig. S4*B*). We previously purified and characterized mouse Wnt3a (20, 21), which is 86.5% identical and 92.5% conserved compared with human WNT3, suggesting that these two Wnt proteins act in conserved biological processes. Therefore, we used purified Wnt3a to determine whether FZD7 mediates exogenous Wnt3a signaling in hESCs. To test this possibility, we used hESCs carrying a WNT/β-catenin-responsive promoter driving expression of a reporter gene encoding green fluorescent protein (GFP). This reporter, referred to as TOP (*Tcf* optimal promoter)-GFP, and similar WNT/β-catenin reporter elements are inactive, or poorly active, in hESCs and become activated on differentiation toward mesendodermal fates (9, 12, 13, 22). Treatment with FZD7-Fab, which effectively binds FZD7 (Fig. 2*D* and Fig. S2), a candidate receptor transducing the Wnt3a signal, did not activate the GFP reporter (Fig. 5 *A*–*D*), indicating that FZD7-Fab binding is not sufficient to stimulate downstream signaling events. As expected, treatment of TOP-GFP hESCs with Wnt3a protein led to GFP expression in a significant proportion of

DEVELOPMENTAL BIOLOGY

cells (Fig. 5 *A* and *C*). Pretreatment of hESCs with the FZD7-Fab for 24 h reduced responsiveness of the reporter cells to Wnt3a by 50% (Fig. 5*A*), indicating that FZD7-Fab binding interferes with signaling of Wnt3a through FZD7. The residual activity can be attributed either to incomplete blocking by FZD7-Fab or to expression of a redundantly acting WNT receptor, such as FZD5. The reduction in signaling on FZD7-Fab pretreatment was not observed in HEK293 cells carrying a WNT/β-catenin luciferase reporter (TOP-Flash; Fig. S5), which lack *FZD7* expression (Fig. 2 *B* and *C* and ref. 16).

Treatment of cells with the GSK3 inhibitor CHIR98014 (CHIR), similar to Wnt3a, potently activates the TOP-GFP reporter (Fig. 5 *B* and *D*). However, in contrast to Wnt3a stimulation, pretreatment with FZD7-Fab has no effect on reporter activation by CHIR (Fig. 5*B*). Therefore, FZD7-Fab blocks Wnt/β-catenin signaling upstream of GSK3, most likely by interfering with receptor–ligand interactions.

In contrast to pretreatment with FZD7-Fab, simultaneous addition of Wnt3a or CHIR and FZD7-Fab to the TOP-GFP reporter cells produced the same amount of reporter activation as Wnt3a or CHIR alone (Fig. 5 *C* and *D*), indicating that FZD7-Fab does not compete with Wnt3a for FZD7 binding. Several mechanisms are possible to explain how FZD7-Fab treatment interferes with FZD7-Wnt3a signal transduction. We found that treatment of hESCs with FZD7-Fab led to a decrease in FZD7 protein (Fig. 5*E*), suggesting it is degraded or that its expression is blocked transcriptionally or translationally. The reduction in FZD7 protein levels is detectable after 4 h of treatment, with a near 50% decline of FZD7 protein levels after 12 h of treatment

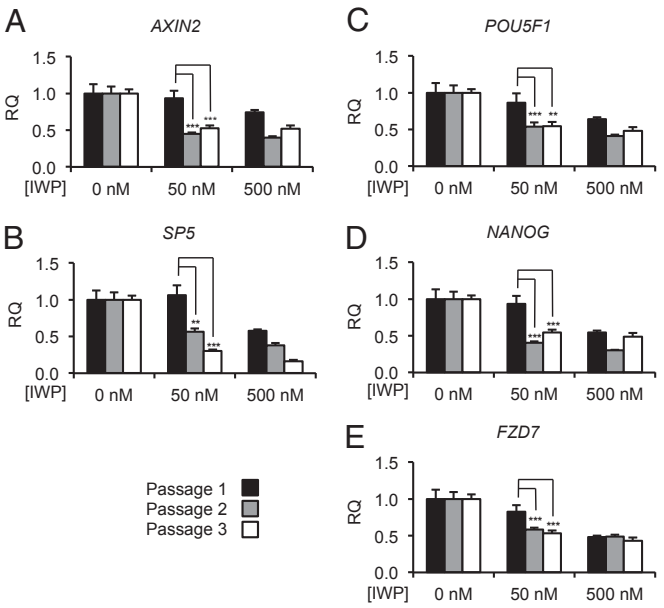

Fig. 6. Blocking endogenous WNT processing reduces expression of pluripotency markers and WNT target genes. HUES9 cells were grown in E8 media with vehicle (DMSO) or with the PORCN inhibitor IWP-2 at the indicated concentrations. Expression of *AXIN2* (*A*), *SP5* (*B*), *POU5F1*/*OCT4* (*C*), *NANOG* (*D*), and *FZD7* (*E*) was determined by qRT-PCR at the indicated passage number (mean ± SEM of four technical samples, normalized to 18S and relative to buffer control). $^{**}P < 0.01$; $^{***}P < 0.001$.

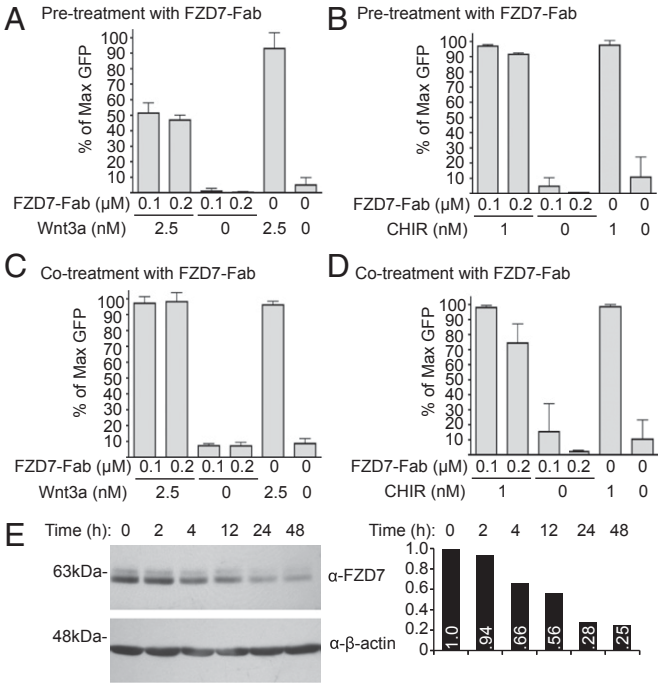

Fig. 5. FZD7-Fab blocks Wnt3a signaling in hESCs. (*A* and *B*) hESCs (HUES9) carrying a Wnt-responsive GFP reporter (TOP-GFP) were pretreated for 24 h with FZD7-Fab at the indicated concentrations and then treated for an additional 24 h with Wnt3a (*A*) or CHIR (*B*–*D*). The TOP-GFP cells were cotreated with FZD7-Fab and either Wnt3a (*C*) or CHIR (*D*) at the indicated concentrations. Fluorescence was quantified by flow cytometry. (*E*) FZD7-Fab treatment of hESCs leads to a decrease in FZD7 protein levels. Cells were treated with FZD7-Fab at a concentration of 0.1 μM for the indicated times. Protein extracts were analyzed by blotting with FZD7-Fab. The bar graph presents quantitation (ImageJ software) of the FZD7 bands shown in the immunoblot.

(Fig. 5*E*). These data suggest that FZD7-Fab leads to FZD7 degradation, potentially through internalization, so that the receptor is no longer available for Wnt3a binding and signaling. FZD7 receptor internalization has also been observed in Wilms' tumor cells treated with anti-FZD7 antibody (23).

The data presented in Figs. 3, 4*A*, and 5 argue for the presence of an endogenous WNT-FZD7 signaling loop required for the maintenance of hESCs in an undifferentiated state. To address this possibility, we examined the effect of blocking endogenous WNT protein with an inhibitor of WNT processing (IWP2), an inhibitor of porcupine (PORCN) (24), an enzyme that processes WNT by attaching a lipid moiety before secretion. Treatment of hESCs with IWP2 led to decreased expression of the WNT target genes *AXIN2* and *SP5* (Fig. 6 *A* and *B*), consistent with the notion that an endogenous WNT signaling pathway is active in hESCs. Furthermore, this treatment led to marked reduction in expression of the pluripotency markers *OCT4*/*POU5F1* and *NANOG* (Fig. 6 *C* and *D*). Importantly, over the course of this IWP treatment, as observed with FZD7-Fab treatment (Fig. 4*A*), *FZD7* expression declined (Fig. 6*E*), lending additional support to the possibility that this cell surface molecule is functionally important for the maintenance of hESCs in an undifferentiated state. It should be noted that this effect of IWP2 on expression of these pluripotency markers was most striking when cells were cultured in the completely defined Essential 8 (E8) medium (25), which is devoid of all WNT proteins or agonists. In contrast, the widely used mTeSR (Stemcell Technologies Inc.) medium contains lithium (1 mM LiCl) (26), which inhibits GSK3 activity and thereby leads to WNT signal activation. Likewise, mouse embryonic fibroblasts (MEFs) and MEF-conditioned medium, which are commonly used for growth of hESCs, could potentially provide WNT proteins and agonists, thereby obfuscating effects of inhibition of WNT protein secretion from hESCs. Therefore, the endogenous FZD7/WNT signaling loop, which we postulate is required to maintain hESCs in an undifferentiated state, is only inhibited by IWP2 when all sources of exogenous WNT activity are eliminated.

Discussion

It is well established that WNT/β-catenin signaling maintains stem cell populations in an undifferentiated state. However, the role of this pathway in human pluripotent stem cell biology remains contentious. Using several lines of evidence, we demonstrated that an endogenous WNT-FZD7 signaling pathway is required to maintain hESCs in an undifferentiated state. First, we showed that the WNT receptor *FZD7* is highly expressed in undifferentiated hESCs, hinting that this receptor may be transducing a WNT signal. Second, using two independent methods to disrupt FZD7 function (shRNA-mediated knockdown and a FZD7-specific Fab), we showed that this WNT receptor is critical to maintain hESCs in an undifferentiated state. This finding is further supported by our observation that treatment of cells with a PORCN inhibitor, which disrupts endogenous WNT processing and secretion, also reduces the pluripotency of hESCs. Third, blocking FZD7 function with the FZD7-Fab blocks WNT signaling by exogenously added Wnt3a protein. Although the FZD7-Fab directly binds to FZD7, it does not compete for binding with Wnt3a but, rather, leads to a decline of FZD7 protein. Taken together, these findings argue that an endogenous WNT-FZD7 signaling pathway operates to maintain hESCs in an undifferentiated state. In addition to *FZD7*, other *FZD* genes, including *FZD5* and *FZD3*, may also act in this pathway, as suggested by their expression in undifferentiated cells relative to differentiated cells. Additional studies are needed to explore the role of other *FZD* genes in these processes.

The identity of the endogenous WNT ligand signaling through FZD7 remains unknown. Genome-wide expression profiling (RNA-seq) identified *WNT3* as the most abundantly transcribed *WNT* gene in hESCs, consistent with publicly available expression data sets [e.g., the Gene Expression Atlas (19)]. In addition, several members of the *RSPO* gene family, which encode secreted molecules that augment WNT signaling activity (27–29), are expressed in hESCs. *WNT3* expression was found to be variable among various hESC lines, with highest relative levels of expression correlating with a propensity to differentiate into endodermal derivatives (14). Together with our finding that FZD7-Fab specifically blocks signaling by Wnt3a, it is likely that WNT3, which is highly conserved to Wnt3a, constitutes a self-renewal ligand interacting with FZD7 in hESCs. A functional connection between FZD7 and WNT3 has also been suggested to exist in hepatic cells (30). However, other WNT ligands may act redundantly with WNT3 and functionally interact with FZD7 to contribute to hESC self-renewal. A definitive identification of the critical WNT ligand will require quantitative affinity measurements between WNTs and their FZD receptors.

Other studies have indicated that hESCs have low levels of endogenous WNT signaling and that active WNT signaling enhances endodermal differentiation propensity (14, 22). Using a WNT-responsive reporter element to monitor endogenous WNT signaling activity, Blauwkamp and colleagues observed the presence of both WNT^{high} and WNT^{low} hESC populations, with the WNT^{high} population leaning toward an endodermal fate (22). We did not observe WNT reporter activity in hESCs carrying a WNT-responsive GFP reporter, a difference that likely stems from the high degree of heterogeneity among distinct hESC lines. In support of this explanation, a recent study found that levels of *WNT3* expression correlate with the propensity of hESCs to differentiate into definitive endoderm (14). Therefore, we propose, as suggested by studies in the hematopoietic system (31), that low WNT signaling activity is required for the maintenance of an undifferentiated state, whereas elevated WNT signaling activity shuttles cells toward mesendodermal fates, consistent with WNT's role in the initiation of gastrulation (32). Furthermore, our data showing that FZD7-Fab blocks endogenous and exogenous WNT signaling while having no effect on mesendodermal differentiation suggest that FZD7 function is dedicated to the maintenance of the pluripotent state and does not mediate the effect of high Wnt signaling activity on mesendodermal differentiation. We speculate that other WNT receptors, such as FZD3 and/or FZD5, which are expressed in undifferentiated hESCs, mediate WNT-induced mesendodermal differentiation. Additional studies are needed to address this possibility.

Exogenous WNT stimulation induces differentiation of hESCs into mesendodermal lineages (12, 13), and treatment of undifferentiated hESCs with a canonical WNT protein or a GSK3 inhibitor has become an established method for inducing definitive endoderm (18, 33–35). These observations, combined with our current findings, suggest that WNT acts as a morphogen, with low levels of signaling promoting hESC self-renewal and high levels inducing endodermal differentiation. Such morphogen activities are well-established in other systems, especially in flies, where Wingless (a *Drosophila melanogaster* Wnt homolog) has distinct activities at high local concentrations versus low distant concentrations (reviewed in ref. 36). Exploiting these morphogen activities of WNT proteins, as well as other developmental signaling molecules such as FGF, sonic hedgehog (SHH), and TGF-β, will likely be critical in differentiating specific cell types from hESCs. In a recent study, this WNT morphogen activity has been used to assign a specific rostro-caudal positional identity to neural progenitor cells derived from hESCs (37).

Our findings demonstrate that FZD7 marks undifferentiated hESCs and that its expression is functionally important for the maintenance of the pluripotent state. This discovery adds to the expanding repertoire of cell surface molecules required for hESC self-renewal, including FGF, insulin-like growth factor (IGF), and epidermal growth factor (EGF) receptors (38–40), E-cadherin (41–44), and L1 cell adhesion molecule (45). Therefore, the cellular machinery regulating hESC pluripotency is not restricted to nuclear factors such as OCT4, NANOG, and SOX2 but is directly influenced by signals originating from the cell surface. Reagents, such as FZD7-Fab described here, may provide powerful tools to isolate and enrich cells with pluripotent properties.

In addition to the observation that *FZD7* expression is increased in undifferentiated human pluripotent stem cells, *FZD7* expression has been associated with several types of cancer, hinting at a possible function in cancer stem cells (23, 46–50). These studies have led to significant interest in FZD7 as a cancer stem cell marker, the targeting of which may be of therapeutic value in the treatment of cancers in which WNT signaling is deregulated (51). The specific FZD7 binding protein (FZD7-Fab), which blocks FZD7 function, as well as Wnt3a signaling, may represent an effective method to disrupt WNT-FZD7 signaling in cancer cells.

Materials and Methods

Cell Lines and Culture Conditions. All media components are from Life Technologies unless indicated otherwise. Mouse embryonic fibroblast (MEF), HEK293, and HEK293T cells were cultured in 1× high glucose DMEM, 10% (vol/vol) FBS, and 1% (vol/vol) L-glutamine penicillin/streptomycin. hESCs HUES9, HUES6, and HUES16 and human induced pluripotent stem cell lines (52) were cultured in 1× DMEM-F12, 20% (vol/vol) Knockout Serum Replacement, 1% (vol/vol) nonessential amino acids, 0.5% (vol/vol) glutamine, 120 μM 2-mercaptoethanol (Sigma). H1/WA01 cells were cultured in E8 medium (25). hESC lines were maintained on feeder layers of mitotically inactivated MEFs ($2 \times 10^4/cm^2$; Millipore) or on Matrigel (BD Biosciences) with MEF conditioned media. MEF conditioned media was produced by culturing hESC medium on MEFs for 24 h, followed by sterile filtering. Plasmids for FZD7 knockdown and overexpression are provided in *SI Materials and Methods*.

RNA and Protein Analysis. Gene expression was analyzed by qRT-PCR. Details on reagents for gene expression analysis are provided in *SI Materials and Methods*. Protein analysis by flow cytometry or immunoblotting followed standard methods detailed in *SI Materials and Methods*.

High-Throughput RNA Sequencing. Total RNA from H1 (WA01; National Institutes of Health Stem Cell Registration Number 0043) was depleted of genomic DNA and rRNA. After ligating the Adaptor Mix, fragmented RNA was converted to the first strand cDNA by ArrayScript Reverse Transcriptase (Ambion), size selected (100–200 bp) by gel electrophoresis, and amplified by PCR, using adaptor-specific primers. Deep sequencing was performed on an Illumina HiSeq2000. Differential gene expression analysis of RNA-seq experiments was performed with TopHat and Cufflinks, as previously described (53, 54). Briefly, raw reads were quality filtered, mapped, and aligned to the reference human genome (hg19) with TopHat. Finally, Cuffdiff was used to calculate gene expression levels as reads per thousand transcript bases per million reads mapped (RPKM). Statistically significant differences in gene expression were calculated from RPKM values.

ACKNOWLEDGMENTS. We are grateful to Eric O'Connor and Karl Marquez in the University of California, San Diego, Human Embryonic Stem Cell Core Facility for assistance with flow cytometry and hESC protocols. This work was supported by a grant from the CIRM (RB1-01406, to K.W.) and the University of California, San Diego, Stem Cell Program and was made possible in part by the California Institute for Regenerative Medicine (CIRM) Major Facilities Grant (FA1-00607) to the Sanford Consortium for Regenerative Medicine. I.J.H. is a recipient of the CIRM Training Grant fellowship for predoctoral candidates (TG2-01154).

1. Merrill BJ (2012) Wnt pathway regulation of embryonic stem cell self-renewal. *Cold Spring Harb Perspect Biol* 4(9):a007971.
2. Nusse R (2008) Wnt signaling and stem cell control. *Cell Res* 18(5):523–527.
3. Reya T, Clevers H (2005) Wnt signalling in stem cells and cancer. *Nature* 434(7035): 843–850.
4. Sokol SY (2011) Maintaining embryonic stem cell pluripotency with Wnt signaling. *Development* 138(20):4341–4350.
5. Anton R, Kestler HA, Kühl M (2007) Beta-catenin signaling contributes to stemness and regulates early differentiation in murine embryonic stem cells. *FEBS Lett* 581(27): 5247–5254.
6. Ogawa K, Nishinakamura R, Iwamatsu Y, Shimosato D, Niwa H (2006) Synergistic action of Wnt and LIF in maintaining pluripotency of mouse ES cells. *Biochem Biophys Res Commun* 343(1):159–166.
7. Sato N, Meijer L, Skaltsounis L, Greengard P, Brivanlou AH (2004) Maintenance of pluripotency in human and mouse embryonic stem cells through activation of Wnt signaling by a pharmacological GSK-3-specific inhibitor. *Nat Med* 10(1):55–63.
8. Singla DK, Schneider DJ, LeWinter MM, Sobel BE (2006) wnt3a but not wnt11 supports self-renewal of embryonic stem cells. *Biochem Biophys Res Commun* 345(2): 789–795.
9. ten Berge D, et al. (2011) Embryonic stem cells require Wnt proteins to prevent differentiation to epiblast stem cells. *Nat Cell Biol* 13(9):1070–1075.
10. Hanna J, et al. (2010) Human embryonic stem cells with biological and epigenetic characteristics similar to those of mouse ESCs. *Proc Natl Acad Sci USA* 107(20): 9222–9227.
11. Tesar PJ, et al. (2007) New cell lines from mouse epiblast share defining features with human embryonic stem cells. *Nature* 448(7150):196–199.
12. Bakre MM, et al. (2007) Generation of multipotential mesendodermal progenitors from mouse embryonic stem cells via sustained Wnt pathway activation. *J Biol Chem* 282(43):31703–31712.
13. Davidson KC, et al. (2012) Wnt/β-catenin signaling promotes differentiation, not self-renewal, of human embryonic stem cells and is repressed by Oct4. *Proc Natl Acad Sci USA* 109(12):4485–4490.
14. Jiang W, Zhang D, Bursac N, Zhang Y (2013) WNT3 Is a Biomarker Capable of Predicting the Definitive Endoderm Differentiation Potential of hESCs. *Stem Cell Rev* 1(1):46–52.
15. Kemp CR, et al. (2007) Expression of Frizzled5, Frizzled7, and Frizzled10 during early mouse development and interactions with canonical Wnt signaling. *Dev Dyn* 236(7): 2011–2019.
16. Melchior K, et al. (2008) The WNT receptor FZD7 contributes to self-renewal signaling of human embryonic stem cells. *Biol Chem* 389(7):897–903.
17. Sperger JM, et al. (2003) Gene expression patterns in human embryonic stem cells and human pluripotent germ cell tumors. *Proc Natl Acad Sci USA* 100(23):13350–13355.
18. Brafman DA, Phung C, Kumar N, Willert K (2013) Regulation of endodermal differentiation of human embryonic stem cells through integrin-ECM interactions. *Cell Death Differ* 20(3):369–381.
19. Kapushesky M, et al. (2012) Gene Expression Atlas update—a value-added database of microarray and sequencing-based functional genomics experiments. *Nucleic Acids Res* 40(Database issue):D1077–D1081.
20. Willert K, et al. (2003) Wnt proteins are lipid-modified and can act as stem cell growth factors. *Nature* 423(6938):448–452.
21. Willert KH (2008) Isolation and application of bioactive Wnt proteins. *Methods Mol Biol* 468:17–29.
22. Blauwkamp TA, Nigam S, Ardehali R, Weissman IL, Nusse R (2012) Endogenous Wnt signalling in human embryonic stem cells generates an equilibrium of distinct lineage-specified progenitors. *Nat Commun* 3:1070.
23. Pode-Shakked N, et al. (2011) Resistance or sensitivity of Wilms' tumor to anti-FZD7 antibody highlights the Wnt pathway as a possible therapeutic target. *Oncogene* 30(14):1664–1680.
24. Chen B, et al. (2009) Small molecule-mediated disruption of Wnt-dependent signaling in tissue regeneration and cancer. *Nat Chem Biol* 5(2):100–107.
25. Chen G, et al. (2011) Chemically defined conditions for human iPSC derivation and culture. *Nat Methods* 8(5):424–429.
26. Ludwig TE, et al. (2006) Feeder-independent culture of human embryonic stem cells. *Nat Methods* 3(8):637–646.
27. Nam JS, Turcotte TJ, Smith PF, Choi S, Yoon JK (2006) Mouse cristin/R-spondin family proteins are novel ligands for the Frizzled 8 and LRP6 receptors and activate beta-catenin-dependent gene expression. *J Biol Chem* 281(19):13247–13257.
28. Binnerts ME, et al. (2007) R-Spondin1 regulates Wnt signaling by inhibiting internalization of LRP6. *Proc Natl Acad Sci USA* 104(37):14700–14705.
29. Kim KA, et al. (2008) R-Spondin family members regulate the Wnt pathway by a common mechanism. *Mol Biol Cell* 19(6):2588–2596.
30. Nambotin SB, Tomimaru Y, Merle P, Wands JR, Kim M (2012) Functional consequences of WNT3/Frizzled7-mediated signaling in non-transformed hepatic cells. *Oncogenesis* 1:e31.
31. Luis TC, et al. (2011) Canonical wnt signaling regulates hematopoiesis in a dosage-dependent fashion. *Cell Stem Cell* 9(4):345–356.
32. Liu P, et al. (1999) Requirement for Wnt3 in vertebrate axis formation. *Nat Genet* 22(4):361–365.
33. D'Amour KA, et al. (2005) Efficient differentiation of human embryonic stem cells to definitive endoderm. *Nat Biotechnol* 23(12):1534–1541.
34. Kroon E, et al. (2008) Pancreatic endoderm derived from human embryonic stem cells generates glucose-responsive insulin-secreting cells in vivo. *Nat Biotechnol* 26(4): 443–452.
35. Schulz TC, et al. (2012) A scalable system for production of functional pancreatic progenitors from human embryonic stem cells. *PLoS ONE* 7(5):e37004.
36. Cadigan KM (2002) Regulating morphogen gradients in the Drosophila wing. *Semin Cell Dev Biol* 13(2):83–90.
37. Kirkeby A, et al. (2012) Generation of regionally specified neural progenitors and functional neurons from human embryonic stem cells under defined conditions. *Cell Rep* 1(6):703–714.
38. Dvorak P, et al. (2005) Expression and potential role of fibroblast growth factor 2 and its receptors in human embryonic stem cells. *Stem Cells* 23(8):1200–1211.
39. Eiselleova L, et al. (2009) A complex role for FGF-2 in self-renewal, survival, and adhesion of human embryonic stem cells. *Stem Cells* 27(8):1847–1857.
40. Wang L, et al. (2007) Self-renewal of human embryonic stem cells requires insulin-like growth factor-1 receptor and ERBB2 receptor signaling. *Blood* 110(12):4111–4119.
41. Eastham AM, et al. (2007) Epithelial-mesenchymal transition events during human embryonic stem cell differentiation. *Cancer Res* 67(23):11254–11262.
42. Li L, et al. (2010) A unique interplay between Rap1 and E-cadherin in the endocytic pathway regulates self-renewal of human embryonic stem cells. *Stem Cells* 28(2): 247–257.
43. Ullmann U, et al. (2007) Epithelial-mesenchymal transition process in human embryonic stem cells cultured in feeder-free conditions. *Mol Hum Reprod* 13(1):21–32.
44. Xu Y, et al. (2010) Revealing a core signaling regulatory mechanism for pluripotent stem cell survival and self-renewal by small molecules. *Proc Natl Acad Sci USA* 107(18): 8129–8134.
45. Son YS, et al. (2011) Brief report: L1 cell adhesion molecule, a novel surface molecule of human embryonic stem cells, is essential for self-renewal and pluripotency. *Stem Cells* 29(12):2094–2099.
46. Gurney A, et al. (2012) Wnt pathway inhibition via the targeting of Frizzled receptors results in decreased growth and tumorigenicity of human tumors. *Proc Natl Acad Sci USA* 109(29):11717–11722.
47. Merle P, et al. (2005) Oncogenic role of the frizzled-7/beta-catenin pathway in hepatocellular carcinoma. *J Hepatol* 43(5):854–862.
48. Nambotin SB, et al. (2011) Pharmacological inhibition of Frizzled-7 displays anti-tumor properties in hepatocellular carcinoma. *J Hepatol* 54(2):288–299.
49. Vincan E, Flanagan DJ, Pouliot N, Brabletz T, Spaderna S (2010) Variable FZD7 expression in colorectal cancers indicates regulation by the tumour microenvironment. *Dev Dyn* 239(1):311–317.
50. Yang L, et al. (2011) FZD7 has a critical role in cell proliferation in triple negative breast cancer. *Oncogene* 30(43):4437–4446.
51. King TD, Zhang W, Suto MJ, Li Y (2012) Frizzled7 as an emerging target for cancer therapy. *Cell Signal* 24(4):846–851.
52. Warren L, et al. (2010) Highly efficient reprogramming to pluripotency and directed differentiation of human cells with synthetic modified mRNA. *Cell Stem Cell* 7(5): 618–630.
53. Trapnell C, et al. (2012) Differential gene and transcript expression analysis of RNA-seq experiments with TopHat and Cufflinks. *Nat Protoc* 7(3):562–578.
54. Trapnell C, et al. (2010) Transcript assembly and quantification by RNA-Seq reveals unannotated transcripts and isoform switching during cell differentiation. *Nat Biotechnol* 28(5):511–515.

Supporting Information

Fernandez et al. 10.1073/pnas.1323697111

SI Materials and Methods

Cell Lines and Culture Conditions. HEK293-TOP (*Tcf* optimal promoter)-Flash were generated by transfection of a plasmid carrying a Super 8× TOP-Flash cassette and a plasmid carrying the gene conferring Neomycin resistance (plasmid ratio, 10:1), and drug-selected clones were isolated and screened for maximal responsiveness (luciferase activity) to Wnt3a stimulation. To generate the TOP-GFP reporter line, HUES9 cells were infected with a lentivirus carrying a 7×Tcf-eGFP/simian virus 40 promoter-puromycin resistance gene (SV40-PuroR) cassette.

Human embryonic stem cells (hESCs) were routinely passaged with Accutase (Millipore), washed, and replated at a density of $4.25 \times 10^4/cm^2$. Genomic integrity of hESCs and genetically modified lines was confirmed by cytogenetic analysis on 20 metaphase cells, using standard protocols for G-banding (Cells Line Genetics).

For IWP treatment (Fig. 6), HUES9 cells were maintained in E8 medium (1) on BD Matrigel-coated (BD Biosciences) tissue culture dishes. Culture medium was supplemented daily with either DMSO or inhibitor of WNT processing 2 (IWP2) (2) solution to a final concentration of 0.1% (vol/vol). IWP-2 solutions of 50 and 500 μM were prepared fresh from a frozen stock at the beginning of each passage. When cells reached 85% confluence, cells were dissociated with Accutase and seeded onto fresh Matrigel-coated plates at a density of 11,000 cells/cm^2 with the Rock inhibitor Y-27632 (10 μM) and either DMSO or IWP-2 at the same concentration in which they were previously cultured.

RNA Analysis. Total RNA was extracted using NucleoSpin RNA II kit (Machery-Nagel) according to manufacturer's instructions. A microgram of RNA was reverse-transcribed, using qScript cDNA Supermix (Quanta Biosciences), and subsequently, 1 μL of template was used per PCR. SensiFAST SYBR Hi-Rox real-time PCR reactions (Bioline) were performed in triplicate, using a CFX96 PCR machine (Bio-Rad) and 40 cycles of amplification (95 °C, 5 s; 60 °C, 15 s). PCR primers (Table S1) were designed using Primer3 software. The specificity of the primers was obtained with a denaturation curve analysis (55–98 °C), resulting in a single peak. Gene expression was normalized to either EF1a or RNA18S5 levels, as indicated. Ct values were obtained with Bio-Rad CFX Manager software, and Delta Ct values were calculated, with a final analysis done in MS Excel (Microsoft).

Protein Analysis. HEK293 cells were transiently transfected with expression vectors carrying FZD cDNAs, using a polyethylenimine (PEI)-mediated transfection method. For immunoblot analysis, cells (HEK293 and hESCs) were washed with PBS and lysed on ice with 1% Triton X-100, 150 mM NaCl, and 50 mM Tris·Cl at pH 7.5. Twenty micrograms of total protein lysate (as determined by Bradford assay) were resolved by SDS/PAGE, transferred to Nitrocellulose (Bio-Rad), probed with FZD7-fragment antigen binding (Fab) (Alere), and detected with HRP-conjugated anti-mouse IgG-HRP (Santa Cruz Biotechnology), using chemiluminescence reagents (Perkin-Elmer Western Lightning ECL) and autoradiography.

For flow cytometry of FZD7, hESCs (HUES 9 and HUES 16) cells were grown to confluency, dissociated with Accutase (Life Technologies), and passed through a cell strainer to remove cell aggregates. For analysis of overexpressed FZD7 in HEK293 by flow cytometry, cells were dissociated with Trypsin-0.25% EDTA (Life Technologies). Unfixed cells were stained with FZD7-Fab (Allere), followed by a R-phycoerythrin-cyanine dye 7 (PE-Cy7)-conjugated rat anti-mouse Ig, kappa light chain (BD Biosciences). Flow cytometry was performed on a FACS Canto II (BD Biosciences). Data were acquired using BD FACSDiva and analyzed using FlowJo software (Tree Star).

For isolation of cell populations with high and low levels of FZD7 cell surface expression by fluorescence-based cell sorting, Accutase-dissociated HUES9 cells were labeled as described earlier and sorted using a FACS Aria 2 (BD Biosciences). Total RNA from sorted cells was subsequently analyzed as described earlier.

Blocking Wnt3a Signaling With FZD7-Fab. For the pretreatment experiments (Fig. 5 *A* and *B*; Fig. S5*A*), FZD7-Fab was added to HUES9-TOP-GFP or HEK293-TOP-Flash cells for 24 h. At that point, cells were treated with either Wnt3a (generated as described in ref. 3) or CHIR98014 (Axon Medchem) for an additional 24 h in the presence of FZD7-Fab. Reporter activity was determined by flow cytometry (TOP-GFP) on a BD FACS Canto 2 or by luminescence detection (TOP-Flash) on a Perkin-Elmer Envision multimode plate reader. In cotreatment experiments (Fig. 5 *C* and *D*; Fig. S5*B*), HUES9-TOP-GFP or HEK293-TOP-Flash cells were treated for 24 h with FZD7-Fab and Wnt3a or CHIR98014 and then analyzed as described earlier.

Plasmids. The following plasmids were used in these studies:

Wnt-Luciferase reporter: Super 8x TOP-Flash, provided by R.T. Moon (University of Washington, Seattle) (4).

Wnt-GFP reporter: 7xTcf-eGFP/SV40-PuroR cassette (Addgene Plasmid 24305, 7TGP) (5).

FZD7 shRNAs, obtained from The RNAi Consortium:

shRNA#1: TRCN0000008343

shRNA#2: TRCN0000008344

shRNA#3: TRCN0000008345

shRNA#4: TRCN0000008346

shRNA#5: TRCN0000008347

FZD overexpression vectors:

FZD1: transferred from pOBT7 (Thermo Scientific, Clone ID 4874253) into pAsiet.

FZD2: transferred from pCR4-TOPO (Thermo Scientific, Clone ID 8322454) into pAsirt.

FZD3: isolated by PCR from cDNA of HUES7-NPCs and cloned into pCI.

FZD4: pLX304 (DNASU Plasmid Repository, Clone ID HsCD00443502).

FZD5: inserted into vector pPGK-CAS (original clone obtained from Thermo Scientific, Clone ID 40011265, modified by site-directed mutagenesis to correct internal stop codon).

FZD7: cloned into pCDNA3.1.

FZD8: gateway cloning from pENTR223.1 (DNASU Plasmid Repository, Clone ID HsCD00082676) into pEF5FR-TV5.

FZD9: gateway cloning from pENTR221 (DNASU Plasmid Repository, Clone ID HsCD00045391) into pEF5FR-TV5.

FZD10: transferred from pBluescriptR (Thermo Scientific, Cone ID 30337870) into pAsiet.

1. Chen G, et al. (2011) Chemically defined conditions for human iPSC derivation and culture. *Nat Methods* 8(5):424–429.
2. Chen B, et al. (2009) Small molecule-mediated disruption of Wnt-dependent signaling in tissue regeneration and cancer. *Nat Chem Biol* 5(2):100–107.
3. Willert KH (2008) Isolation and application of bioactive Wnt proteins. *Methods Mol Biol* 468:17–29.
4. Veeman MT, Slusarski DC, Kaykas A, Louie SH, Moon RT (2003) Zebrafish prickle, a modulator of noncanonical Wnt/Fz signaling, regulates gastrulation movements. *Curr Biol* 13(8):680–685.
5. Fuerer C, Nusse R (2010) Lentiviral vectors to probe and manipulate the Wnt signaling pathway. *PLoS ONE* 5(2):e9370.
6. Warren L, et al. (2010) Highly efficient reprogramming to pluripotency and directed differentiation of human cells with synthetic modified mRNA. *Cell Stem Cell* 7(5):618–630.

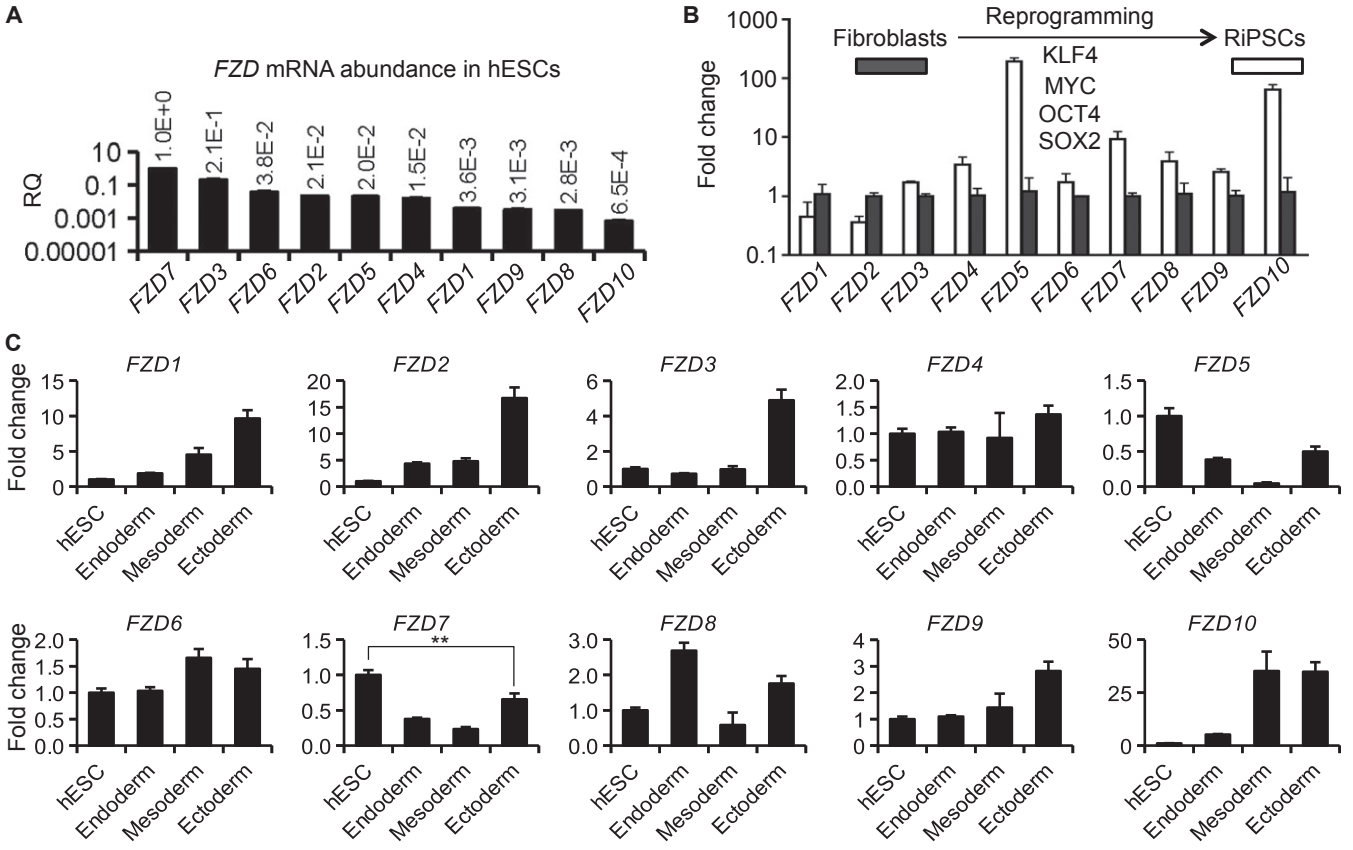

Fig. S1. Related to Fig. 1. FZD7 expression is elevated in undifferentiated relative differentiated cells. (*A*) Expression of all *FZD* genes in hESCs (HUES9). Expression of all *FZD* genes was determined by quantitative reverse transcription PCR (qRT-PCR). Consistent with RNA-seq data presented in Fig. 1*A*, *FZD7* is amplified most efficiently relative to all other *FZD* genes. RQ, relative quantity. (*B*) Up-regulation of *FZD7* on cellular reprogramming. *FZD7* expression is up-regulated as human foreskin fibroblasts (BJ, American Type Culture Collection) are reprogrammed to an induced pluripotent stem cell state (BJ-induced pluripotent stem cell lines), using modified RNA transcripts for KLF4, OCT4, and SOX2 (6). *EF1A* was used as a normalization control. (*C*) *FZD7* expression is increased in undifferentiated hESCs vs. cell populations with ecto-, endo-, and mesodermal phenotypes. Among the other 9 *FZD* genes, only *FZD5* mirrors the expression of *FZD7*. Data are represented as mean ± SD of three technical samples, normalized to *EF1a* and relative to undifferentiated hESCs. $^{**}P < 0.01$.

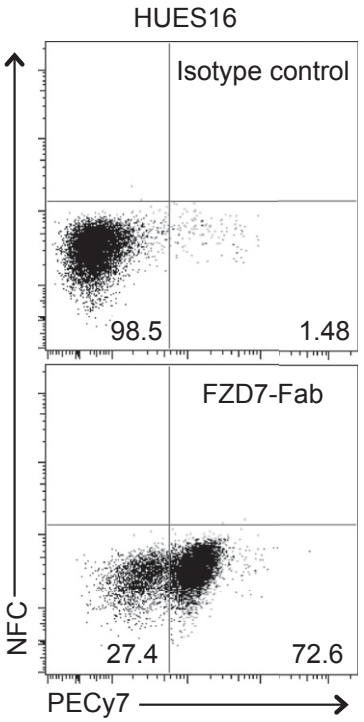

Fig. S2. Related to Fig. 2D. FZD7 is expressed on hESCs. FZD7-Fab specifically reacts with an antigen displayed on live HUES16 cells.

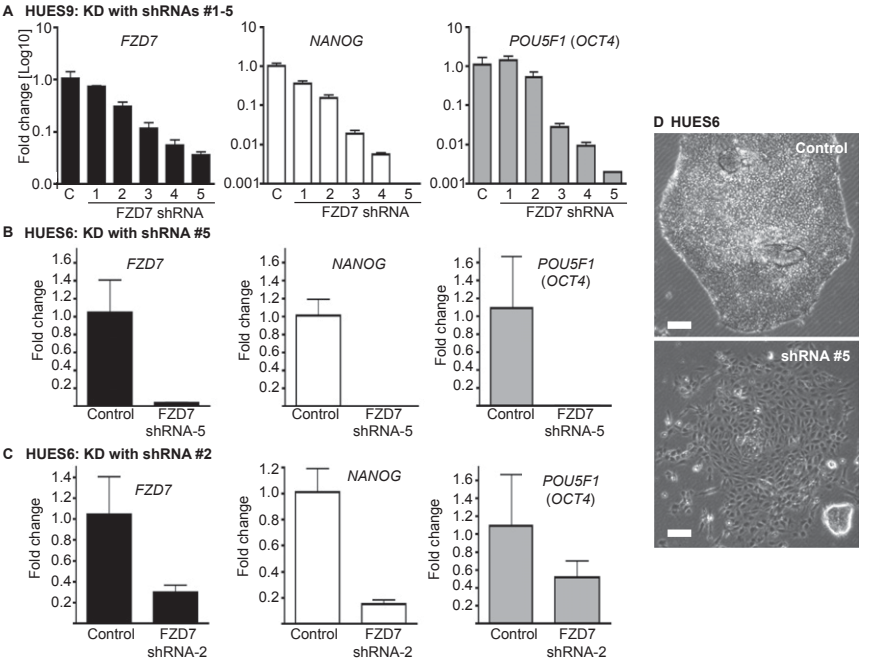

Fig. S3. Related to Fig. 3. Knockdown of FZD7 using lentiviral delivery of shRNAs disrupts pluripotency of hESCs. (*A*) Five distinct shRNAs designed to target the FZD7 transcript (RNAi Consortium Library) were transduced into HUES9, and expression of the genes *FZD7*, *NANOG*, and *POU5F1*/*OCT4* was determined using qRT-PCR. (*B*) HUES6 cells were transduced with shRNA 5 and expression of *FZD7*, *NANOG*, and *POU5F1*/*OCT4* was determined using qRT-PCR. (*C*) HUES6 cells were transduced with shRNA 2, and expression of *FZD7*, *NANOG*, and *POU5F1*/*OCT4* was determined using qRT-PCR. *EF1A* was used as a normalization control. (*D*) HUES6 cells with knockdown of *FZD7* by shRNA 5 lose their characteristic cell morphology.

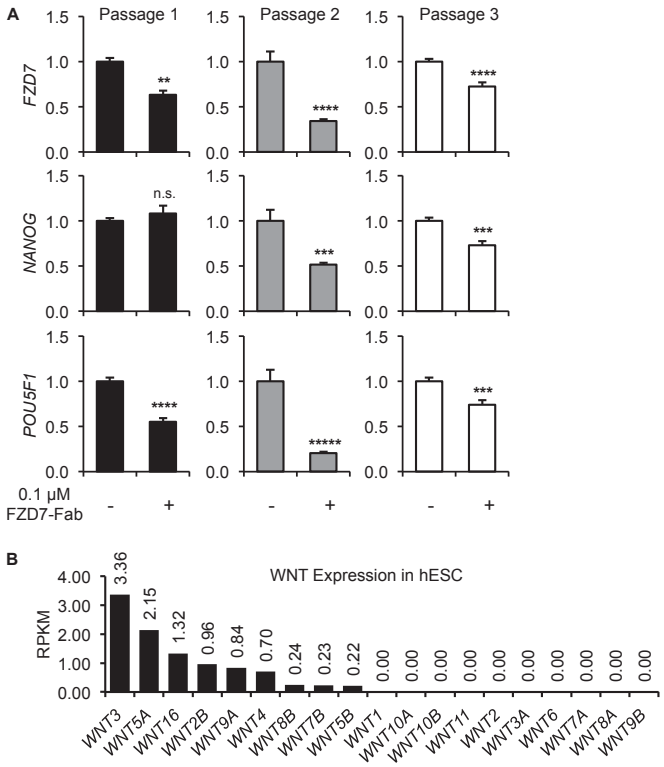

Fig. S4. Related to Fig. 4. Treatment of hESCs with FZD7-Fab disrupts expression of pluripotency markers. (*A*) hESCs (H1/WA01) were cultured in the presence or absence of FZD7-Fab over 3 passages. At each passage, gene expression levels of *FZD7* and the pluripotency regulators *POU5F1*/*OCT4* and *NANOG* was determined by qRT-PCR (mean ± SD of three technical samples, normalized to 18S and relative to untreated control). $^{**}P < 0.01$; $^{***}P < 0.001$; $^{****}P < 0.0001$; $^{*****}P < 0.00001$; n.s. not statistically significant. (*B*) Characterization of *WNT* gene expression. *WNT3* is the most abundantly expressed *WNT* gene in hESCs (H1/WA01). Gene expression levels for all 19 *WNT* genes were calculated from RNA-seq data as reads per thousand transcript bases per million reads mapped (RPKM).

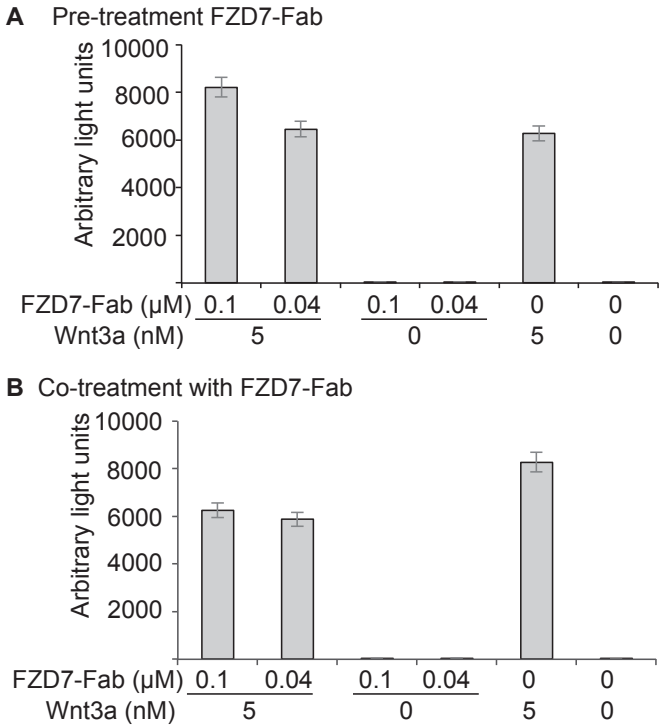

Fig. S5. Related to Fig. 5 *A* and *C*. FZD7-Fab does not interfere with Wnt3a signaling in HEK293 cells. HEK293 cells carrying the WNT/β-catenin reporter TOP-Flash were pretreated (*A*) or not pretreated (*B*) with FZD7-Fab for 24 h at the indicated concentrations. Cells were then treated with Wnt3a with and without FZD7-Fab for an additional 24 h, and cell lysates were analyzed for luciferase activity. In contrast to HUES9-TOP-GFP cells, FZD7-Fab did not block Wnt3a activity in HEK293-TOP-Flash cells.

Table S1. List of primers used for qRT-PCR analysis

Gene name	Forward primer	Reverse primer
AXIN2	TATCCAGTGATGCGCTGACG	CGGTGGGTTCTCGGGAAATG
FZD1	CTACCACTTCCTGGGGGAGA	CACAGCACTGACCAAATGCC
FZD2	TTTCTGGGCGAGCGTGAT	AAACGCGTCTCCTCCTGTGA
FZD3	GGATCGGTGTTTTCAGCATT	TGCAGCGTTCTTGTATCCAC
FZD4	GGCGGCATGTGTCTTTCAGT	GAATTTGCTGCAGTTCAGACTCTCT
FZD5	ACACCCGCTCTACAACAAGG	CTCAGGATAGCGGAAGCGTT
FZD6	ACAAGCTGAAGGTCATTTCCAAA	GCTACTGCAGAAGTGCCATGAT
FZD7	TTCTCGGACGATGGCTACC	GAACCAAGTGAGAGACAGAATGACC
FZD8	GGAGTGGGGTTACCTGTTGG	GTAGCCGATGCCCTTACACA
FZD9	GCCTGTGCTACCGCAAGATA	GTTCTCCAAAGAGGGGTCCG
FZD10	GCTCAAGTGCTCCCCGATTA	GCCTCCATGCACAGGTAGTT
EEF1A1	CTGGAGCCAAGTGCTAACATG	CCGGGTTTGAGAACACCAGT
RNA18S5	GTAACCCGTTGAACCCCATT	CCATCCAATCGGTAGTAGCG
NANOG	TTTGTGGGCCTGAAGAAAACT	AGGGCTGTCCTGAATAAGCAG
POU5F1	CTTGAATCCCGAATGGAAAGGG	GTGTATATCCCAGGGTGATCCTC
SOX1	GGCTTTTGTACAGACGTTCCC	AACCCAAGTCTGGTGTCAGC
SOX17	GTGGACCGCACGGAATTTG	GGAGATTCACACCGGAGTCA
SP5	TCGGACATAGGGACCCAGTT	CTGACGGTGGGAACGGTTTA
T	CTATTCTGACAACTCACCTGCAT	ACAGGCTGGGGTACTGACT

Primer sequences are given by convention 5′ to 3′.